Materiały Wysokoenergetyczne / High Energy Materials, ***2019***, *11 (1), 95 − 102; DOI: 10.22211/matwys/0120E*
ISSN 2083-0165

Research paper / Praca doświadczalna

Study of the effect the rate of addition of the antisolvent on the crystallization of the CL-20
Badanie wpływu szybkości dozowania nierozpuszczalnika na przebieg krystalizacji CL-20

Joanna Szczygielska[1, *)], Paweł Maksimowski[2)], Wincenty Skupiński[2)]

[1)] *Institute of Industrial Organic Chemistry**, 6 Annopol Street, 03-236 Warsaw, Poland*
[2)] *Faculty of Chemistry, Warsaw University of Technology, 3 Noakowskiego Street, 00-664 Warsaw, Poland*
**E-mail:* szczygielska@ipo.waw.pl
*** now called: Łukasiewicz Research Network – Institute of Industrial Organic Chemistry*

Abstract: *In this paper, the effect of antisolvent addition rate on the yield and polymorphic purity of the obtained product, in order to optimise the 2,4,6,8,10,12-hexanitro-2,4,6,8,10,12-hexaazaisowurtzitane (CL-20) precipitation process using a solvent/antisolvent system, was determined.*
It was found that increased dispensing rate of the antisolvent results in increased supersaturation in the mother liquor. This, in turn, increases the nucleation rate. The prevalence of the process of creating new seeds reduces the growth rate of the crystal, which affects the size distribution of the final crystallisation product. Reducing the time of the process results in the transformation of the initially formed, kinetically stable polymorph β, into the thermodynamically stable ε form with a lower yield, than the yield obtained after increased time.
Streszczenie: *W niniejszej pracy w ramach optymalizacji procesu krystalizacji 2,4,6,8,10,12-heksanitro–2,4,6,8,10,12-heksazaizowurcytanu (CL-20) metodą wytrącania z układu rozpuszczalnik/nierozpuszczalnik, określono wpływ szybkości dozowania nierozpuszczalnika na wydajność oraz czystość polimorficzną otrzymywanego produktu.*
Podsumowując rezultaty badań stwierdzono, że im szybciej dozowany jest nierozpuszczalnik tym większe jest, generowane w roztworze macierzystym, przesycenie, co w efekcie przekłada się na zwiększenie szybkości nukleacji. Przewaga procesu tworzenia nowych zarodków powoduje zmniejszenie szybkości wzrostu kryształów, co ma wpływ na rozkład ziarnowy finalnego produktu krystalizacji. Krótszy czas prowadzenia procesu powoduje, że powstała, jako pierwsza forma, kinetycznie stabilna – β ulega w mniejszym stopniu transformacji do formy stabilnej termodynamicznie – ε, niż ma to miejsce przy dłuższym czasie prowadzenia procesu.

Keywords: *ε-CL-20, antisolvent crystallization, polymorphic purity*
Słowa kluczowe: *ε-CL-20, krystalizacja przez wytrącanie, czystość polimorficzna*

1. Introduction

Crystallisation of CL-20 is used to obtain crystals of appropriate quality in terms of the application of the material in a formulation. The quality of crystals can be defined by the following parameters [1]:

– crystal shape and dimensions,
– chemical and polymorphic purity,
– defects content,
– sensitivity to mechanical stimuli,
– thermal stability, and
– compatibility.

It is well understood that a carefully selected crystallisation technique and optimal process conditions have a significant effect on the quality of the obtained product.

The most frequently indicated technique for crystallisation of CL-20 is the precipitation from a solvent/antisolvent system [2-7]. An alternative method involves crystallisation by evaporation, in which the generated supersaturated solution is controlled by the solvent removal rate [8, 9]. An advantage of precipitation with an antisolvent is the ability to conduct the process at low temperatures, which helps to avoid the $\varepsilon \rightarrow \gamma$ temperature transformation likely to occur during the evaporation of liquid solvents. On the other hand, crystallisation from a solvent/antisolvent system is associated with high nucleation rate, which may promote the growth of the most kinetically stable β-CL-20 variant [1]. Moreover, the speed and location of antisolvent addition, as well as appropriate mixing dynamics are the leading parameters controlling the supersaturation in the crystalliser volume. These parameters have a direct effect on the properties of the obtained crystals; therefore, the optimisation of CL-20 crystallisation is based on an experimental selection and a strict control of the conditions of the process in question.

Based on literature, it is known that the same solvent/antisolvent system may generate various polymorphs depending on the conditions of the crystallisation process [10]. According to Foltz *et al.* [11, 12] the β form can be transformed into the γ form and then into the ε form by selecting an appropriate solvent and recrystallisation temperature. As a result of the transformation, the crystal density changes from 1.98 g/cm^3 for the β form, to 2.044 g/cm^3 for the ε form.

The dependence of the precipitation process yield on the crystallisation system used should be based on the CL-20 solubility data in the solvent/antisolvent system. Reference [10] presents solubility in selected crystallisation systems. However, these data are only valid for the selected solvent/antisolvent ratios at two temperatures and do not provide information on the CL-20 solubility curves in the described systems.

The selection of parameters determining the generated supersaturation, *i.e.* the concentration of the antisolvent in time, temperature, number of the ε variety seeds, allows achieving the target size distribution of a high-energy material [13]. The existence of defects in the crystal structure of CL-20 is a unavoidable phenomenon resulting from the growth of crystals under various conditions. Obtaining CL-20 seeds with specific morphology and sizes, containing the smallest possible number of defects, results in reduced sensitivity to mechanical stimuli [14, 15]. In the current work, the antisolvent dosage rate parameter in the CL-20 crystallisation process using the ethyl acetate/chloroform system was optimised. The influence of the rate of generated supersaturation on the quality of the crystals obtained in the process was determined.

2. Materials and methods

During the research, CL-20 obtained from TADNOIW at the Institute of Energetic Materials at the Warsaw University of Technology, and analysis-pure (a.p.) chemical reagents were used. The solubility tests of CL-20 were performed in an ethyl acetate/chloroform system. The measuring set consisted of a 100 cm^3 flask, a thermometer, a water bath and a magnetic stirrer with a heating plate. Measurements were carried out at temperatures of 25, 30 and 40 °C at a mixing speed of 300 rpm. A specific amount of CL-20 was weighed out into the flask using an analytical balance (accuracy up to four decimal places). The CL-20 flask with the weighed

amount was placed in a water bath, and the solvent/antisolvent mixture with volumetric composition, which was determined for the given experiment, was added in 0.1 cm^3 portions. The proportions of ethyl acetate and chloroform are given in Table 1. A 10 min break was allowed between each addition, after which it was determined by visual inspection whether the precipitate had completely dissolved. The test was continued until a clear solution was obtained. Each measurement was repeated three times.

Table 1. The volume ratio of ethyl acetate/chloroform mixture

Ethyl acetate/chloroform	1/4	2/3	1/1	3/2	7/3	9/1	1/0

Measurements were also conducted to determine the CL-20 supersaturation curve in the ethyl acetate/chloroform system. The tests were carried out in a measuring set analogous to the solubility test system. To obtain various concentrations of CL-20 in the solvent/antisolvent mixtures, different weighed amounts of CL-20 in the range of 100-400 mg were used, which were always dissolved in 2 cm^3 of ethyl acetate. The CL-20 solution was added to a 100 cm^3 volumetric flask, thermostated at 25 °C and stirred. Chloroform was then added in portions of 0.1 cm^3. Following each addition, a waiting period of 10 min was carried out, after which it was determined by visual inspection whether a precipitate had formed. The test was continued until the solution became cloudy. Each measurement was repeated three times.

Crystallisation tests were carried out at various antisolvent dosage rates in the system, which consisted of a 250 cm^3 reactor equipped with a mechanical stirrer with speed control, a peristaltic pump, and a thermometer. The tests were carried out at a temperature of 25 °C. A solution of 5 g CL-20 dissolved in 13 cm^3 of ethyl acetate was added to the reactor. 60 cm^3 of the antisolvent were added dropwise at a specified rate. The precipitate was filtered under reduced pressure, washed with methanol and air dried. Table 2 presents parameters of the conducted series of tests on the CL-20 crystallisation.

Table 2. Crystallisation parameters in the ethyl acetate/chloroform system

Sample	Antisolvent dosage rate [cm^3/min]	Process time [h]	Antisolvent to solvent volume ratio
I	0.16	6.0	4.6
II	0.25	4 0	
III	0.50	2.0	
IV	2.00	0.5	

The material obtained as part of the optimisation of the crystallisation process was characterised using available techniques. Infrared sample spectra were recorded in the 400-4000 cm^{-1} range using a Nicolet 6700 camera. The crystallographic purity of the ε-CL-20 variety was calculated using formula (1) determined based on the calibration curve of the relationship between X_ε and the height ratio of the I_{820}/I_{880} peaks in the spectrum part called the "fingerprint region".

$$X_\varepsilon = 2.224 \cdot (I_{820}/I_{880}) - 0.0676 \quad (1)$$

The chemical purity of CL-20 was determined using a Shimadzu liquid chromatograph (Japan), which consisted of an LC-10AD pump, an SPD-10A UV detector and a CTO-10A oven. The separation was carried out using a LiChroCART Purspher RP-18 5 µm 125x4 mm column and a 5 × 4 mm pre-column with the same packing. Chemical purity was calculated from the peak areas of the obtained chromatograms. The gradient procedure was used for the analysis, and a mixture of water and THF was used as the mobile phase. Detection was carried out at 254 nm. Specific density was determined using an automatic helium pycnometer – AccuPyc II 1340. Pictures of the crystals were taken using an optical microscope (Eduko, type SK 392) in combination with an Olympus camera, model C560. The IPS-U (Infrared Particle Sizer) version 8.12 analyser was used to measure the size distribution of crystals obtained in the crystallisation process.

3. Results of the experiments

3.1. Solubility of CL-20 in the ethyl acetate/chloroform system

This study attempts to estimate the width and location of the CL-20 metastable zone for the ethyl acetate/chloroform system. For this purpose, solubility and saturation curves were determined. Fig. 1 shows the CL-20 metastable zone in this system.

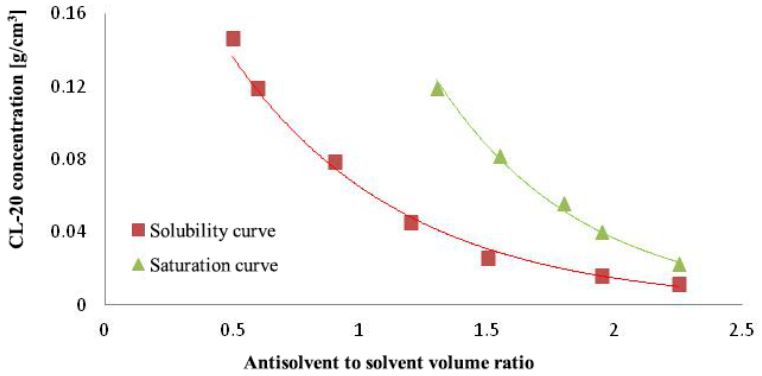

Figure 1. CL-20 metastable zone area in the ethyl acetate/chloroform system

The concentration range of CL-20 within the zone area is 0.01-0.15 mol/dm^3 for the ratio of antisolvent to solvent in the range of 0.5-2.5. The zone area is stretched over a wide range of CL-20 concentrations. Increasing the ratio of antisolvent to solvent from 0.5:1 to 2.5:1 causes a significant decrease in the solubility of CL-20 in this system. Due to the low solubility of CL-20 in this system, the nucleation process starts with a 1.25-fold excess of the antisolvent relative to the solvent.

3.2. Study on the influence of chloroform dosage rate on the crystallisation process

Optimal process parameters, at which the crystal growth occurs in a way that they do not contain inclusions of the basal solution or any other defects, must be determined experimentally. Therefore, a series of crystallisations was carried out using basic process parameters in the ethyl acetate/chloroform system, with changes in the dosage rate of the antisolvent, in other words, the rate of generated supersaturation. Table 3 presents the results of the conducted tests.

Table 3. The results of crystallisation in ethyl acetate (15 cm^3)/chloroform (70 cm^3) depending on the dosage rate of the antisolvent (300 rpm, temperature 25 °C)

Sample	Antisolvent dosage rate [cm^3/min]	Yield [%]	Density [g/cm^3]	Chemical purity [%]	Crystal ε purity [%]
I	0.16	82	2.030	98	93
II	0.25	80	2.025	98	87
III	0.50	83	2.019	97	83
IV	2.00	85	2.008	98	68

The yield of the CL-20 crystallisation using the ethyl acetate/chloroform system, regardless of the dosage rate of the antisolvent, is 80-85%. The chemical purity of the obtained samples is equal to approximately 98%. The polymorphic purity of the obtained material decreases as the dosage rate of the antisolvent increases.

The decrease in the content of the ε variety is reflected in the density of the crystals, the value of this parameter drops from 2.030 g/cm^3 to 2.008 g/cm^3.
Fig. 2 shows the FT-IR spectra of samples obtained during crystallisation I and IV in the 800-900 cm^{-1} range. The peaks characteristic for the ε variety, marked in the figure at 820 cm^{-1}, differ in height due to the difference in the content of this polymorphic variety.

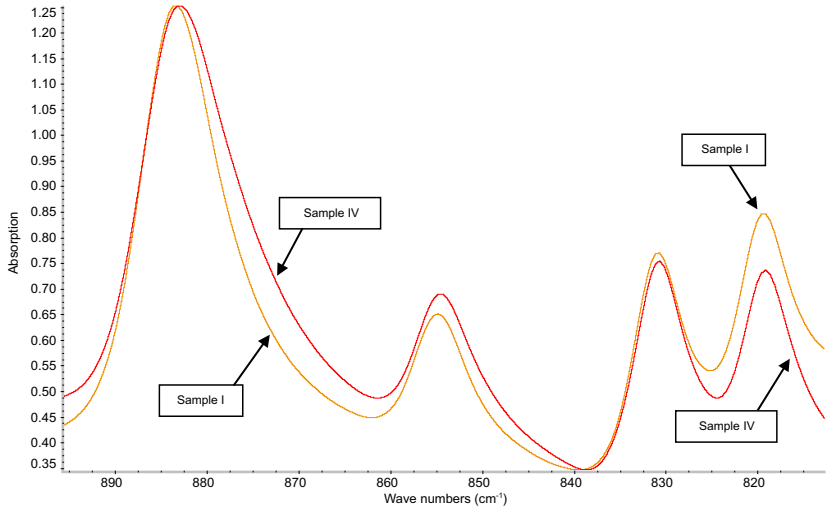

Figure 2. FT-IR spectrum in the "fingerprint" region of samples I and IV

The granulometric distributions of the obtained CL-20 samples were determined. Fig. 3 presents a comparison of seed size ranges precipitated during individual crystallisations.

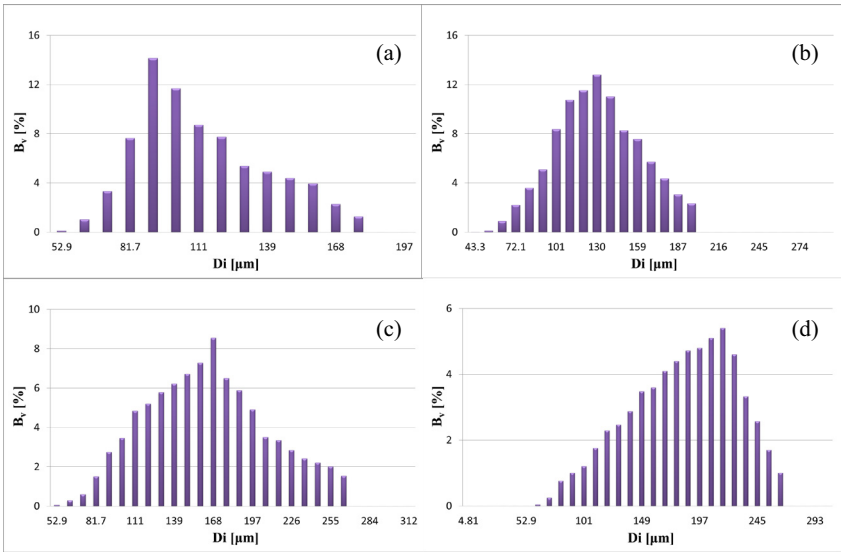

Figure 3. Changes in the volume fraction of individual CL-20 crystal fractions depending on the antisolvent dosing rate: (a) 2.00 cm^3/min, (b) 0.50 cm^3/min, (c) 0.25 cm^3/min, (d) 0.16 cm^3/min

The use of a higher antisolvent dosing rate, namely 2.00 cm^3/min, results in seed sizes in the range of 50-180 μm, with the most numerous fraction at 90 μm. By reducing the addition rate of the precipitation agent to 0.5 cm^3/min, the particle size range extends to 190 μm and the maximum fraction includes the crystals with a size of 130 μm. The CL-20 sample formed during the precipitation process, when the antisolvent was dosed at a rate of 0.25 cm^3/min is in the range 50-260 μm, with a predominant fraction at 170 μm. Extending the crystallisation process time to 6 h, thereby reducing the antisolvent dosing rate to 0.16 cm^3/min leads to an extension of the CL-20 particle size range to 280 μm, with the largest fraction size of 220 μm. Fig. 4 presents the morphology of the CL-20 crystals obtained in the conducted tests.

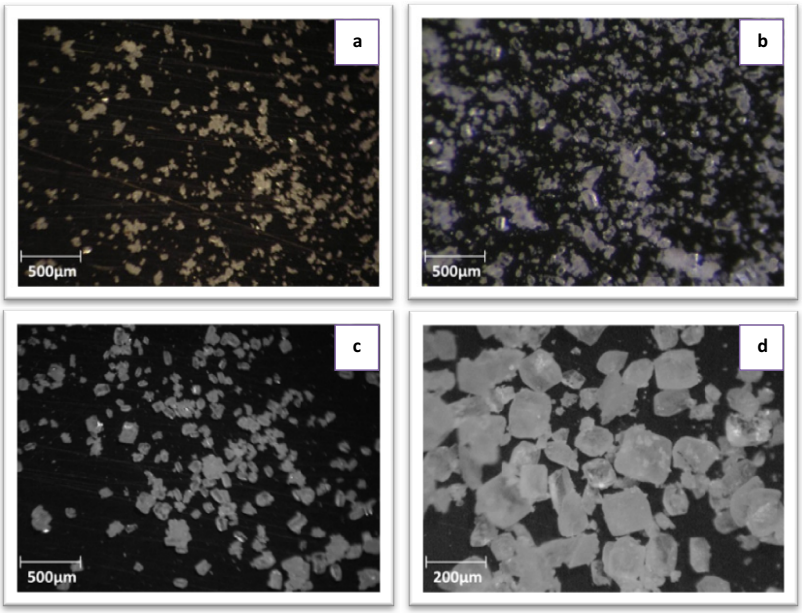

Figure 4. The morphology of the CL-20 crystals obtained during crystallisations carried out at different antisolvent dosing rates: (a) 2.00 cm^3/min, (b) 0.50 cm^3/min, (c) 0.25 cm^3/min, (d) 0.16 cm^3/min

Based on the optical analysis of the crystals, it can be determined that the shape of the seeds obtained in all samples are cuboid with rounded corners. Therefore, it can be concluded that the antisolvent dosing rate has no effect on the shape of the CL-20 crystals.

4. Results and discussion

As part of this study, the effect of the antisolvent dosing rate on the course of CL-20 crystallisation in the ethyl acetate/chloroform system, was investigated. In order to optimise the crystallisation process, the width of the metastable CL-20 zone in the given crystallisation system was experimentally determined. The crystallised substance remains in solution until a sufficiently high level of supersaturation is achieved with the aim of spontaneous nucleation. During the investigation of the metastable area, it was found that due to the low solubility of CL-20 in this system, the nucleation process already takes place at a 1.25-fold excess of the antisolvent relative to the solvent.

As part of the tests, CL-20 samples with chemical purity of approximately 98% were obtained. The yield of the crystallisation process in ethyl acetate/chloroform is at a constant (within the experimental error) level of 80-85%. The CL-20 crystallisation series shows that extending the dosing time for a specific amount of the antisolvent does not lead to a significant increase in the process efficiency. However, this parameter affects

the efficiency of obtaining ε-CL-20. Along with increasing the chloroform dosing rate, a decrease in polymorphic purity and density of the obtained CL-20 crystals was observed. The short duration of the process means that not all of the initially formed β variety seeds had sufficient time to dissolve; therefore, a decrease in crystallographic purity is observed. This conclusion can be confirmed on the basis of analogous observations presented in [16]. This phenomenon can be explained based on the Ostwald's Rule, according to which, under given conditions, the least stable and most soluble variety crystallizes first [17], gradually changing to more thermodynamically stable and less soluble polymorphs [18]. As a result, crystals of a thermodynamically stable variety are formed in the solution, and all precursors, so called the metastable phase, are dissolved. In addition, this rule states that larger crystals form as a result of the dissolution of small crystals. This is due to the value of interfacial energy, which is the decisive factor in the kinetics and thermodynamics of the nucleation process. Small crystals exhibit higher solubility and lower surface tension; therefore, they precipitate first and are the «fuel» for the formation of larger crystals [19, 20].

By analysing the sizes of crystals obtained in this series of tests, it can be further concluded that extending the crystallisation time, while reducing the antisolvent dosing rate, affects the extension of the CL-20 crystal size range. In addition, a shift in the volume share of the most numerous fraction of the obtained samples is observed. When dosing the antisolvent at a rate of 2.00 cm^3/min, the 90 μm fraction is the largest volume fraction, while at a dosing rate of 0.16 cm^3/min, the 220 μm fraction is the most abundant.

5. Summary

The work examined the impact of the solvent dosing rate on the quality of the CL-20 crystals obtained in the precipitation process. Summary of the research results allows the conclusion to form that the faster the antisolvent is dosed, the greater the local supersaturation generated in the mother liquor, which in turn translates into an increase in the rate of nucleation. The predominance of created new seeds causes a decrease in the crystal growth rate, which affects the particle size distribution of the final crystallisation product. Confirmation for this hypothesis can be found in literature [21-23]. Shorter process time means that the resulting first kinetically stable form – β – is transformed into the thermodynamically stable form to a lesser extent than it is in the case of a longer process time, which in turn translates into polymorphic purity of the obtained product. Based on the series of tests, it was noted that under the test conditions the optimal, due to the polymorphic purity of the obtained product, dosing rate of the non-solvent was 0.16 cm^3/min for the process carried out in 6 h.

Acknowledgements

The research was carried out as part of a project financed by the Ministry of Science and Higher Education, Project No. NN 209 084038.

References

[1] Teipel U. 2005. *Energetic Materials. Crystallization.* Wiley-VCH, 53-132.

[2] Bouma H.B.R., Duvalois W., van der Heijden E.D.M.A., Steen A.C. 2000. *Characterization of a commercial grade CL-20 morphology, crystal shape, sensitivity and shock initiation testing by flyer impact. Int. Conf. ICT, Proc.,* Karlsruhe, June 27-30.

[3] van der Heijden E.D.M.A., Bouma H.B.R. 2004. Crystallization and Characterization of RDX, HMX, and CL-20. *Cryst. Growth Des.* 4 (5): 999-1007.

[4] Bescond P., Graindorge H., Mace H.. 1999. *Antisolvent-Solvent Crystallization of Hexanitrohexaazaiso-wurtzitane to Obtain the ε-Polymorph.* European Patent Application 91337A1.

[5] Peralta-Inga Z., Degirmenbasi N., Olgun U., Gocmez H., Kalyon M.D. 2006. Recrystallization of CL-20 and HNFX from Solution for Rigorous Control of the Polymorph Type: Part I, Mathematical Modeling using Molecular Dynamics Method. *J. Energ. Mater.* 24 (2): 69-101.
[6] Degirmenbasi N., Peralta-Inga Z., Olgun U., Gocmez H., Kalyon M.D 2006. Recrystallization of CL-20 and HNFX from Solution for Rigorous Control of the Polymorph Type: Part II, Experimental Studies. *J. Energ. Mater.* 24 (2): 103-139.
[7] Sanderson J.A., Hamilton S.R., Warner F.K. 2002. Crystallization of 2,4,6,8,10,12-hexanitro-2,4,6,8,10,12-hexaazatetracyclo[5.5.0.0^{5,9}0^{3,11}]-dodecane. Patent USA 6,350,871 B1.
[8] Ghosh M., Venkatesan V., Sikder K.A., Sikder N. 2012. Preparation and Characterisation of **ε**-CL-20 by Solvent Evaporation and Precipitation Methods*. Def. Sci. J.* 62 (6): 390-398.
[9] Lee M.-H., Kim J.-H., Park Y.-C., Hwang J.-H., Kim W.-S. 2007. Control of Crystal Density of ε-Hexanitrohexaazaisowurzitane in Evaporation Crystallization. *Ind. Eng. Chem. Res.* 46: 1500-1504.
[10] Lapina Yu.T., Savitskii A.S., Motina E.V., Bychin N.V., Lobanova A.A., Golovina N.I. 2009. Polymeric Transformation of Hexanitrohexaazaisowurzitane. *Russ. J. Appl. Chem.* 82: 1821-1828.
[11] Foltz M.F., Coon L.C., Garcia F., Nichols III L.A. 1994. The thermal stability of the polymorphs of hexanitrohexaazaisowurtzitane, Part I. *Propellants Explos. Pyrotech.* 19: 19-25.
[12] Foltz M.F. 1994. Thermal Stability of ε-Hexanitrohexaazaisowurtzitane in an Estane Formulation. *Propellants Explos. Pyrotech.* 19: 63-69.
[13] Schefflana R., Kovenklioglu S., Kalyon D., Redner P., Heider E. 2006. Mathematical Model for a Fed-Batch Crystallization Process for Energetic Crystals to Achieve Targeted Size Distributions. *J. Energ. Mater.* 24: 157-172.
[14] Vaullerin M., Espagnacq A., Morin-Allory L. 1998. Prediction of impact sensitivity. *Propellants Explos. Pyrotech.* 23 (5): 237-239.
[15] Oxley C.J., Smith L.J., Buco R., Huang J. 2007. A Study of Reduced-sensitivity RDX. *J. Energ. Mater.* 25 (3): 141-160.
[16] Kim J.H., Park Y.Ch., Yim Y.J., Han J.-S. 1998. Crystallization Behavior of Hexanitrohexaazaisowurtzitane at 298 K and Quantitative Analysis of Mixtures of Its Polymorphs by FTIR. *J. Chem. Eng. Jpn.* 31: 478-481.
[17] Calmanovici E.C., Biscans B., Gilot B., Laguerie C., Giulietti M. 1996. Stable and Metastable Modifications Relates with Solid Formation from Solutions. *Industrial Crystallization, 13th Symp. Proc.,* Toulouse, France, 349-354.
[18] Giulietti M., Seckler M.M., Derenzo S., Ré I.M., Cekinski E. 2001. Industrial crystallization and precipitation from solutions: state of the technique. *Braz. J. Chem. Eng.* 18 (4): 423-440.
[19] Mullin W.J. 1997. *Crystallization.* Oxford : Butterworth.
[20] Nývlt J. 1995. The Ostwald Rule of Stages. *Cryst. Res. Technol.* 30 (4): 443-449.
[21] Mersmann A. 1994. *Crystallization Technology Handbook.* New York : Marcel Dekker Inc.
[22] Manth T., Mignon D., Offermann H. 1996. The role of hydrodynamics in precipitation. *J. Cryst. Growth* 166: 998-1003.
[23] Mersmann A. 1999. Crystallization and precipitation. *Chem. Eng. Process.* 38: 345-353.

Polish version:
The work was originally published in Polish, in the *High Energy Materials* journal (*Materiały Wysokoenergetyczne*) 2015 (7): 117-124. Polish version is available in PDF-format, in colour, at:
http://www.wydawnictwa.ipo.waw.pl/materialy-wysokoenergetyczne/materialy-wysokoenergetyczne7/HEM_0120.pdf

English version:
– Revised: November 28, 2019
– Published first time online: December 10, 2019